

Calculation of the diffusion coefficient of Au in Bi-2223 superconductors

This article has been downloaded from IOPscience. Please scroll down to see the full text article.

2007 J. Phys.: Condens. Matter 19 346205

(<http://iopscience.iop.org/0953-8984/19/34/346205>)

View [the table of contents for this issue](#), or go to the [journal homepage](#) for more

Download details:

IP Address: 129.252.86.83

The article was downloaded on 29/05/2010 at 04:27

Please note that [terms and conditions apply](#).

Calculation of the diffusion coefficient of Au in Bi-2223 superconductors

O Ozturk¹, T Küçükömeröglü² and C Terzioglu¹

¹ Department of Physics, Faculty of Arts and Sciences, Abant İzzet Baysal University, 14280 Bolu, Turkey

² Department of Physics, Faculty of Arts and Science, Karadeniz Technical University, 61080 Trabzon, Turkey

Received 27 April 2007, in final form 8 June 2007

Published 20 July 2007

Online at stacks.iop.org/JPhysCM/19/346205

Abstract

Undoped Bi-2223 samples were prepared using a conventional solid-state reaction method. Doping of Au in Bi-2223 was carried out by means of diffusion from an evaporated Au film on pellets. We have investigated the effect of Au diffusion and diffusion-annealing duration on the microstructure and superconducting properties of Au-doped samples by performing x-ray diffraction (XRD), scanning electron microscopy (SEM), dc resistivity and critical current density measurements. Gold diffusion in $\text{Bi}_{1.8}\text{Pb}_{0.35}\text{Sr}_{1.9}\text{Ca}_{2.1}\text{Cu}_3\text{O}_y$ has been studied over the temperature range 500–800 °C using the technique of successive removal of thin layers and the measurements of lattice parameters from XRD patterns at room temperature. The diffusion doping of Bi-2223 by Au causes a significant increase of the lattice parameter c by about 0.19%. This observation is used for calculation of the Au diffusion coefficient in Bi-2223. The Au diffusion coefficient decreases as the diffusion-annealing temperature decreases. The temperature dependence of the Au diffusion coefficient in the range 500–800 °C is described by the relation $D = 4.4 \times 10^{-4} \exp(-1.08 \text{ eV}/k_B T)$. Au doping of the sample increased the critical transition temperature and the critical current density from 100 ± 0.2 to 104 ± 0.2 K and from 40 to 125 A cm⁻², in comparison with those of undoped samples. The critical transition temperature and critical current density of Au-doped samples increased with increasing diffusion-annealing time from 10 to 50 h. Au doping of the sample also improved the surface morphology and increased the high- T_c phase ratio. The possible reasons for the observed improvement in superconducting properties of the samples due to Au diffusion are discussed.

(Some figures in this article are in colour only in the electronic version)

1. Introduction

The noble metals such as silver and gold, in the same column as copper in the periodic table, are of special interest for high-temperature superconductors [1]. There has been a tremendous amount of work on Bi(Pb)–Sr–Ca–Cu–O (BSCCO) system since its discovery. To improve the superconducting properties, partial substitution and diffusion have been investigated extensively [1–9]. Görür *et al* [10, 11] investigated the effect of Ag diffusion on the properties of $\text{YBa}_2\text{Cu}_3\text{O}_{7-x}$ (YBCO) thin films produced by electron-beam deposition techniques and bulk samples. They found that, for an Ag-doped sample, the critical transition temperature and the critical current density were increased while the room-temperature resistivity values were decreased in comparison with those of undoped YBCO. The researchers found that Ag addition in the BSCCO system enhances the critical current density (J_c) [12, 13], improves the superconducting transition temperature (T_c) [14, 15], mechanical properties and electrical stability [16], and reduces the normal-state resistivity and the contact resistance [15, 17]. On the other hand, it was observed that Au addition degraded the superconductivity of Bi(Pb)–Sr–Ca–Cu–O [17]. In contrast, it was also found that Au addition did not affect the T_c and lattice parameters [18] and did not affect the formation of Bi-2223 [19]. Therefore, there have been contradictions concerning gold addition. It could be observed that in all of the investigations, the addition of gold to Bi(Pb)–Sr–Ca–Cu–O was carried out in the mixed powders, before the pressing and the sintering of pellets. Dzhafarov *et al* [1] reported the effect of Au diffusion combined with slow and fast cooling on the critical temperature and critical current density in the Bi(Pb)–Sr–Ca–Cu–O system. The gold-diffusion doping of Bi(Pb)–Sr–Ca–Cu–O in the sintering process with a fast cooling promotes formation of the high- T_c Bi-2223 phase, and significant increases in J_c were observed.

The diffusion coefficients of gold may be useful for the understanding of the doping mechanism and changes of microstructure and superconducting properties of BSCCO systems under doping. To our knowledge, no detailed work on the calculation of the Au diffusion coefficient in a Bi(Pb)–Sr–Ca–Cu–O bulk sample has been published in the literature. In the previous studies [20, 21], the effect of Au doping and diffusion-annealing time on mechanical properties (hardness, yield strength, Young's modulus, and fracture toughness) of Bi-2223 was investigated. The investigation indicated that increased Au doping and diffusion-annealing time increased the Vickers hardness, Young's modulus, yield strength, and fracture toughness.

In this paper, we present the results of the influence of Au diffusion and diffusion-annealing time on the lattice parameters, microstructure, and superconducting properties such as critical current density (J_c) and critical transition temperature (T_c) of $\text{Bi}_{1.8}\text{Pb}_{0.35}\text{Sr}_{1.9}\text{Ca}_{2.1}\text{Cu}_3\text{O}_y$ samples. The diffusion parameters of Au defined from the XRD patterns of diffusion-doped Bi(Pb)SrCaCu–Au samples are also presented. The diffusion coefficient is calculated using the technique of successive removal of thin layers and calculation of the lattice parameter c from XRD patterns, at room temperature, for each diffusion-annealing temperature (500, 600, 700, 750, and 800 °C for 10 h).

2. Experimental details

Superconducting $\text{Bi}_{1.8}\text{Pb}_{0.35}\text{Sr}_{1.9}\text{Ca}_{2.1}\text{Cu}_3\text{O}_y$ samples were prepared by the standard solid-state reaction method. Weighed powders of Bi_2O_3 (99.99%), PbO (99.9+%), SrCO_3 (99.9+%), CaCO_3 (99+%) and CuO (99+%) in the cation ratio Bi:Pb:Sr:Ca:Cu = 1.8:0.35:1.9:2.1:3 were mixed by ball milling for 24 h. After the milling, the mixed powders were calcined in air at 700, 750 and 800 °C for 24 h. The sample was cooled to room temperature and ground after calcination. The calcined powder was ground and pressed into pellets of size $10 \times 4 \times 2 \text{ mm}^3$

at 300 MPa. The pellets were sintered in air at 830 °C for 48 h and then cooled down to room temperature. The heating and cooling rates of the temperature were chosen to be 10 and 3 °C min⁻¹, respectively. Doping of Au in Bi-2223 was carried out by means of diffusion from an evaporated Au film on pellets. The Au evaporation (thickness of about 50 μm) on one face of the samples was carried out using an AUTO 306 vacuum coater (EDWARDS). Then, the Au layered superconducting samples were annealed at 830 °C for 10, 20 and 50 h. At the end of this run, Au diffusion was realized through the samples. For comparison, an undoped sample was also annealed under the same conditions. In addition to this, the diffusion annealing process was investigated to calculate the diffusion coefficient of Au. For this reason, virgin bulk samples were coated with an Au layer and diffusion annealing was carried out at 800, 750, 700, 600 and 500 °C for 10 h. The diffusion annealing was performed in a programmable tube furnace from PROTHERM (model PTF 12/75/200). Typical dimensions of the samples for transport, XRD and SEM measurements were 2 × 4 × 10 mm³. After diffusion runs the remaining layers of Au were removed from surfaces of the samples by etching in HCl + H₂O solution for different times to calculate the diffusion coefficient.

The electrical resistivity as a function of temperature between 90 and 130 K and the critical current density at 77 K were measured by a standard dc four-probe method using a closed-cycle cryostat. Both voltage and current contacts were made with silver paint. A Keithley 220 programmable current source and a Keithley 2182A nano-voltmeter were used for the resistivity and *I*-*V* measurements. The transition temperature, *T_c*, was defined as the temperature at which *R* = 0. We determined *J_c* from the *I*-*V* curves at 77 K; the criterion for critical current was 1 μV cm⁻¹.

The surface morphologies of the Au-diffused and pure samples were studied by using a Philips XL30 SFEG scanning electron microscope. SEM micrographs were taken from fracture surfaces of the bulk samples.

The phase evaluation and lattice parameter calculation of the Au-doped and pure samples were analysed by means of a Rigaku D/Max-IIIC x-ray diffractometer with a Cu Kα target giving a monochromatic beam with wavelength 1.54 Å. The spectra were collected in the range 2θ = 4°–60° with a scan speed of 3° min⁻¹ and a step increment of 0.02° at room temperature. The phase purity and the lattice parameters were determined from these XRD patterns. The accuracy in determining the lattice parameter *c* was ±0.001 Å. The mean values of lattice parameter *c* of Bi_{1.8}Pb_{0.35}Sr_{1.9}Ca_{2.1}Cu₃O_{*y*} samples are determined from the high-angle (00*l*) peaks of the XRD measurements.

The relative volume fractions of the Bi-2223 and Bi-2212 phases were determined from the peak intensities of the same particular reflections, using the following expressions [22, 23]:

$$f_{(2223)} = \frac{\sum I_{H(hkl)}}{\sum I_{H(hkl)} + \sum I_{L(hkl)}} \quad (1)$$

$$f_{(2212)} = \frac{\sum I_{L(hkl)}}{\sum I_{H(hkl)} + \sum I_{L(hkl)}}. \quad (2)$$

Here *I_{H(hkl)}* and *I_{L(hkl)}* are the intensities of the (*hkl*) peaks for Bi-2223 and Bi-2212 phases, respectively (figure 1).

The XRD measurements provide data about the lattice parameters for only a thin surface layer of the Au-diffused Bi_{1.8}Pb_{0.35}Sr_{1.9}Ca_{2.1}Cu₃O_{*y*} sample, since the effective penetration depth of the x-rays is about 15 μm into the sample. Hence, information about the diffusion profile of non-uniformly distributed Au in Bi_{1.8}Pb_{0.35}Sr_{1.9}Ca_{2.1}Cu₃O_{*y*} can be obtained by the successive removal of thin layers from the Au-diffused surface of the sample and the measurement of the lattice parameters. It is observed that substitution of matrix atoms by impurity atoms with a different radius causes a deformation near the impurity atoms [24]. This

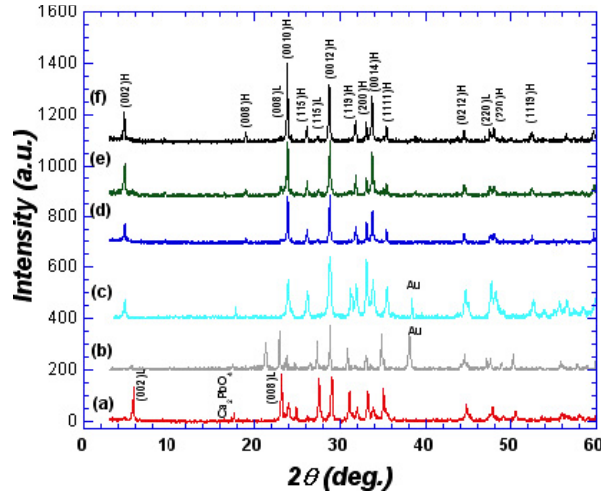


Figure 1. (a) The powder XRD pattern of sample G0, (b) XRD pattern taken from the surface of the Au-covered bulk sample before grinding and annealing, (c) XRD pattern taken from the surface of the bulk sample G1 before grinding (annealed), (d) powder XRD pattern of sample G1, (e) powder XRD pattern of sample G2 and (f) powder XRD pattern of the sample G3. The peaks indexed $(hkl)L$ and $(hkl)H$ represent the Bi-2212 and Bi-2223 phases, respectively.

results in changes of lattice parameters of the specimen. The deformation, ε , in the region of the crystalline lattice at point x is given by

$$\varepsilon(x) = [c(x) - c_0]/c_0, \quad (3)$$

where $c(x)$ and c_0 are the lattice parameters in the deformed and non-deformed region of the samples, respectively. This deformation is related to the radii of impurity and matrix atoms, and also to the concentration of impurity atoms, $N(x)$, namely by the relation

$$\varepsilon(x) = \beta N(x). \quad (4)$$

Here β is the expansion coefficient of the lattice given by [25]

$$\beta = \frac{1}{3N_\ell} \left[1 - \left(\frac{r_i}{r_0} \right)^3 \right], \quad (5)$$

where r_i and r_0 are the radii of the impurity and the matrix atoms, respectively, and N_ℓ is the concentration of the matrix atoms. Thus, data about the concentration profile of the diffusing impurity in the Au-diffused sample can be found by measuring the distribution of deformation ($\varepsilon(x) = \Delta c/c_0$) over the thickness of the samples.

In this study, it is supposed that the conditions of impurity diffusion from a constant source into a semi-infinite solid are satisfied by the following equation [26]:

$$N(x, t) = N_0 [1 - \text{erf}(x/2\sqrt{Dt})] \quad (6)$$

where $\text{erf}[x/2(Dt)^{1/2}]$ represents the error function with argument $y = x/2(Dt)^{1/2}$:

$$\text{erf}(y) = \frac{2}{\sqrt{\pi}} \int_0^y \exp(-y^2) dy. \quad (7)$$

Here $N_0 = N(0, t)$ is the constant concentration on the surface of the sample, $N(x, t)$ is the impurity concentration at the distance x , D is the diffusion coefficient, and t is the diffusion-annealing time.

Table 1. Critical temperature T_c , transition width ΔT_c , transport critical current density J_c , lattice parameter c , volume fraction, and room-temperature resistivity of the samples.

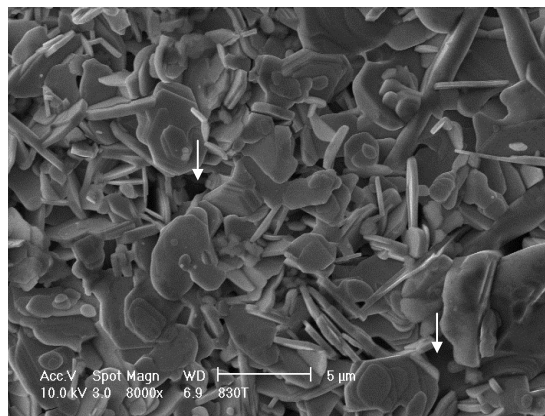
Samples	ΔT_c (K)	T_c^{offset} (K)	Lattice parameter c (Å)	J_c^{trans} (A cm^{-2})	Hole concentration p	Volume fraction (%)		ρ ($\text{m}\Omega \text{ cm}$) at 300 K
						2212	2223	
G0	8	100 ± 0.2	36.960	40	0.126	34	66	8.50
G1	6	104 ± 0.2	37.030	125	0.134	15	85	7.10
G2	5	105 ± 0.2	37.190	135	0.137	11	89	6.70
G3	5	106 ± 0.2	37.206	150	0.139	8	92	6.35

3. Results and discussion

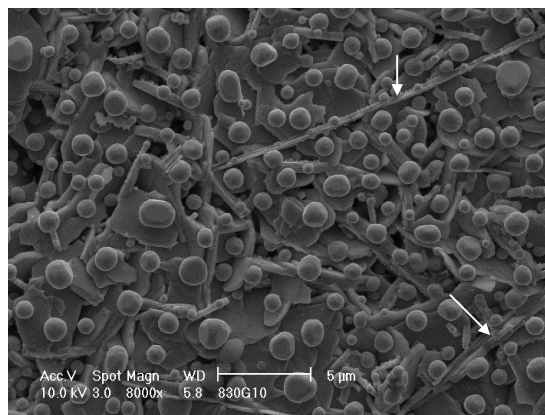
The samples of Bi-2223 pellets will be hereafter denoted as G0 (undoped sample annealed at 830°C for 10 h), G1 (gold-diffused sample annealed at 830°C for 10 h), G2 (gold-diffused sample annealed at 830°C for 20 h), and G3 (gold-diffused sample annealed at 830°C for 50 h). The XRD patterns from the surface of samples G0, G1, G2 and G3 are shown in figure 1. Some of the Miller indices are indicated in the figure. We used the linear least-square method to calculate the lattice parameters of the samples. The determined lattice parameters from the (00 l) peaks of the XRD data are given in table 1. XRD peaks due to Au are not seen in the powder XRD patterns of the diffusion-doped samples (figure 1(d)) although they were seen in the XRD patterns taken from the surface of the bulk samples before grinding (figure 1(c)). The values of the lattice parameter c of sample G1 calculated from the sample's surface (37.100 Å) and from powder (37.030 Å) were compared, and it was found that the c -parameter of the surface is larger. This result implies that Au is incorporated into the structure from the surface by diffusion. Au doping (G1) increased the c -parameter and the intensity of the peaks, and decreased the a -parameter of the sample in comparison with that for the undoped sample (G0), being in agreement with a previous work [1]. The increase in the intensities of the peaks for the G1 sample may testify to the enhanced grain growth and orientation of grains with Au diffusion, causing the critical current density increase, as was confirmed in critical current density measurements. It was observed that the c -parameter increased with further increasing the diffusion-annealing time (20 and 50 h). Our measurements showed an increase of the c -parameter by about 0.19%. We used this information to calculate the diffusion coefficient of Au. The increase in the c -parameter indicated that cations of the system (Bi^{3+} , Sr^{2+} , Ca^{2+}) may partly be substituted by Au ions (0.85 Å). Substitution at the Cu site is less likely because we have observed that T_c of the samples has increased.

The relative volume fraction of the samples calculated using equations (1) and (2) is listed in table 1. As is seen in the table, with Au diffusion, the volume fraction of Bi-2223 phase increased and that of Bi-2212 phase decreased. Diffusion doping of the sample by gold improves the formation of the high- T_c Bi-2223 phase in comparison with undoped sample, as was confirmed by dc resistivity measurements in the present work.

The surface morphology of the gold-doped Bi(Pb)–Sr–Ca–Cu–O was studied by SEM in order to determine the grain sizes and possible precipitation at the grain boundaries. Figure 2 represents surface micrographs for samples G0 and G1. The grain size of sample G1 is relatively bigger than that of sample G0, as shown in figure 2, although we have not carried out a conclusive quantitative analysis. The surface of sample G1 is also smoother and denser. Arrows on the SEM pictures indicate longer grains and voids. The tiny spherical objects on the surface of the micrograph shown in figure 2(b) are gold particles. They are absent in the micrograph shown in figure 2(a). These results indicate that the surface morphology of the



(a)



(b)

Figure 2. SEM micrographs of the (a) G0 and (b) G1 samples.

sample is relatively improved by Au-doping. Sample G0 has non-uniform surface appearance with smaller grains. SEM pictures of the surface of the samples annealed at lower temperatures present completely different morphology. For instance, the sample annealed at 800 °C has small spheres of gold particles disrupting the uniform film appearance, which was observed when the 500 °C-annealed samples were examined. This finding also shows that diffusion of gold at 800 °C is much slower than in the heat treatment of 830 °C. Gold film on the sample forms a metallic connection; this resistive short-circuit connects the grains and lowers the room-temperature resistivity. This effect continues even when the gold film is diffused into the sample, indicating the gold's effect on grain boundary properties. SEM pictures show better connectivity in gold-coated samples after heat treatment at 830 °C for 10 h.

The electrical resistivity was measured using the standard four-probe dc technique, in the temperature range between 90 and 130 K. Room-temperature resistivities were calculated from room temperature I - V curves (table 1). The value of the resistivity at room temperature decreased upon Au doping and annealing time. The temperature dependence of resistivity for all samples (G0, G1, G2 and G3) is shown in figure 3. The temperature dependence of the resistivities of the samples shows metallic behaviour (at $T \geq 110$ K) with the zero-resistivity

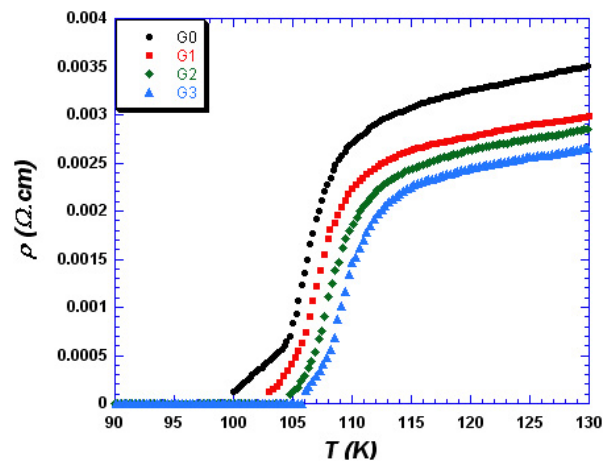


Figure 3. Temperature dependence of resistivity for the undoped (G0) sample annealed at 830 °C for 10 h and Au-doped $\text{Bi}_{1.8}\text{Pb}_{0.35}\text{Sr}_{1.9}\text{Ca}_{2.1}\text{Cu}_3\text{O}_y$ samples annealed at 830 °C for 10 h (G1), 20 h (G2), and 50 h (G3).

transition temperatures of 100 K, 104 K, 105 K and 106 K, respectively. The transition width of the samples decreases with increasing annealing time. The broadening of the transition width shows that sample G0 has a lower percentage of the Bi-2223 phase compared to that of gold-diffused samples. The reduction of broadening in ρ - T curve may be due to the modifying effect of the gold diffusion on the grain boundaries. Sharper transitions are accompanied by higher critical temperature and higher critical current density values.

On the other hand, we have carried out further analysis of the temperature-resistivity data between the G0 and G1 samples. Both samples were annealed isothermally at 830 °C for 10 h. It was obtained that the transition curves from the normal state to the superconducting state have a double-step behaviour, which is more pronounced in G0. We believe that the double-step resistive transition is an indication of weak links and dominance of the Bi-2212 phase. It is observed that the zero-resistivity transition temperature of sample G1 (104 K) is higher than that for sample G0 (100 K), being consistent with a previous work [1]. The increase in T_c may be related to the optimization of the hole concentration and possible changes in the lattice vibration of Bi(Pb)-Sr-Ca-Cu-O. It is also possible that resistive nature of the grain boundaries is modified by accumulation of gold atoms at the grain boundaries, but this requires elucidation by a transmission electron microscopy study, which is part of our plans. Although wetting of the grain boundaries by a very thin layer of gold is unlikely, preferential accumulation of gold ions at the grain boundaries may reduce the resistive behaviour.

The transport critical current density of samples G1 and G0 (annealed under the same conditions) measured in liquid nitrogen are 125 and 40 A cm^{-2} , respectively. It should be noted that the transport critical current density of the gold-doped sample is about three times larger than that of undoped Bi(Pb)-Sr-Ca-Cu-O. A similar increase of J_c was observed in Au-doped Bi(Pb)-Sr-Ca-Cu-O [1] and YBaCuO superconductors [25]. The J_c of gold-coated samples increases with increasing annealing time. The increase of J_c in Bi(Pb)-Sr-Ca-Cu-O by Au diffusion may be caused by the increase of grain sizes and their orientations, by improved coupling between Au-diffused superconducting grains, and by the increased number of flux-pinning centres due to the presence of Au in the intergrain regions. This similar improving effect of Au diffusion on J_c is revealed for the critical transition temperature. The increased value of J_c in sample G1 compared with G0 in our investigations can be interpreted as a result

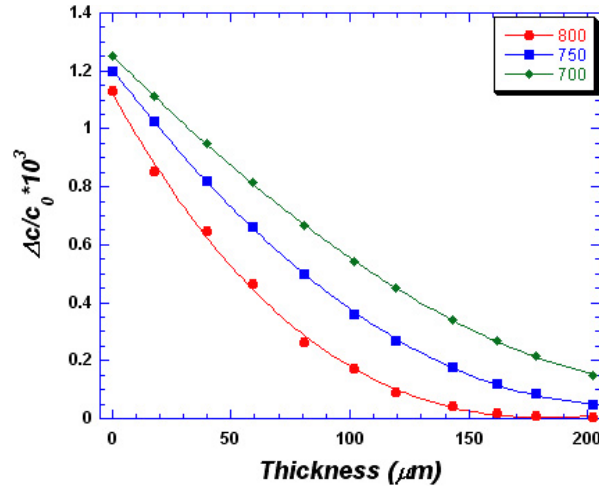


Figure 4. Distribution of deformation $\Delta c/c_0$ versus the thickness of $\text{Bi}_{1.8}\text{Pb}_{0.35}\text{Sr}_{1.9}\text{Ca}_{2.1}\text{Cu}_3\text{O}_y$ diffusion doped by Au at 800, 750, and 700 °C for 10 h (the full curve is calculated according to equation (6)).

of gold diffusion in intergrain boundaries. This in turn causes the increase of intergrain contact surface or decreasing the intergrain resistivity. It is observed that the value of J_c in sample G1 (125 A cm^{-2}) is lower than that of G2 and G3 (135 and 150 A cm^{-2} , respectively) in our investigations. From the above result, it was inferred that the annealing time has a positive effect on the J_c value of the samples. As mentioned before, the c -parameter is increased with increasing diffusion-annealing duration. The longer the average length of the lattice parameter c , the higher J_c becomes. This indicates that an Au-doped Bi-2223 sample has better J_c with the heat treatment schemes employed in the present work.

The carrier (number of holes) concentration, p , is calculated by using the relation [27]

$$T_c/T_c^{\max} = 1 - 82.6(p - 0.16)^2 \quad (8)$$

where T_c^{\max} is taken as 110 K for Bi-2223 system. This formula is found to be applicable to several cuprate systems [2, 28]. The calculated carrier concentration is given in table 1. It is observed that the hole carrier concentration for samples G0 and G1 were 0.126 to 0.134, respectively. Further increasing the diffusion-annealing time from 10 to 50 h increased the (hole) carrier concentration from 0.126 to 0.139. The slight increase in T_c may also be related to the optimization of the hole density. Thus, Au diffusion improves the carrier density by affecting the hole concentration and causing possible changes in the lattice vibration of Bi(Pb)–Sr–Ca–Cu–O.

As was already mentioned above, one would expect that the change of lattice parameter c with the thickness of the samples resembles the concentration distribution of diffusion gold impurity. From this considerations, the change of lattice parameter c was studied by successive removal of thin layers from the sample and by XRD measurements. As mentioned before, Au layers were removed from surfaces of the samples by etching in $\text{HCl} + \text{H}_2\text{O}$ solution for different times. Figure 4 represents the variation of lattice parameter $\Delta c/c_0$ (c_0 is the lattice parameter of the undoped region of the sample) as a function of thickness of the sample, exposed to Au diffusion at 800, 750 and 700 °C for 10 h. The solid curve shows the calculated concentration profile of Au in Bi-2223. The experimental data of figure 4 fit well with the theoretical curve, calculated for $D = 1.2 \times 10^{-8} \text{ cm}^2 \text{ s}^{-1}$ at 800 °C by using equation (6). The

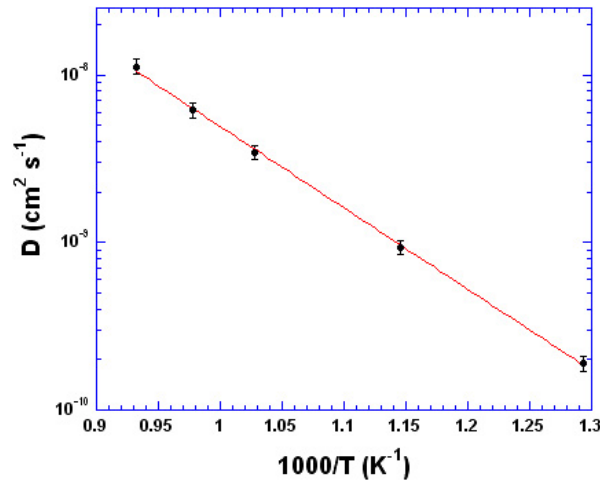


Figure 5. Temperature dependence of Au diffusion coefficient in the $\text{Bi}_{1.8}\text{Pb}_{0.35}\text{Sr}_{1.9}\text{Ca}_{2.1}\text{Cu}_3\text{O}_y$ superconductors.

same fitting method was used for the samples that were diffusion annealed at 500, 600, 700, and 750 °C, and the values of diffusion coefficient were found to be 6.1×10^{-9} for 750 °C, 3.5×10^{-9} for 700 °C, 9.4×10^{-10} for 600 °C and 1.9×10^{-10} for 500 °C. Diffusion at lower temperatures is much less significant, being in agreement with our SEM results given earlier in this paper. The mean values of the diffusion coefficients of Au in $\text{Bi}_{1.8}\text{Pb}_{0.35}\text{Sr}_{1.9}\text{Ca}_{2.1}\text{Cu}_3\text{O}_y$ as a function of temperature are given in figure 5. The results of these studies showed that the Au diffusion coefficient in the $\text{Bi}_{1.8}\text{Pb}_{0.35}\text{Sr}_{1.9}\text{Ca}_{2.1}\text{Cu}_3\text{O}_y$ system in the temperature range 500–800 °C increases in accordance with the Arrhenius relation

$$D = 4.4 \times 10^{-4} \exp\{(-1.08 \pm 0.10) \text{ eV}/k_B T\}. \quad (9)$$

This relatively low value of the activation energy (1.08 eV) of Au in $\text{Bi}_{1.8}\text{Pb}_{0.35}\text{Sr}_{1.9}\text{Ca}_{2.1}\text{Cu}_3\text{O}_y$ may testify that the migration of Au primarily proceeds through defects in the polycrystalline sample (pore surfaces, grain boundaries, etc) as in the case for Au diffusion in YBaCuO ceramics [25].

4. Conclusions

$\text{Bi}_{1.8}\text{Pb}_{0.35}\text{Sr}_{1.9}\text{Ca}_{2.1}\text{Cu}_3\text{O}_y$ samples were prepared using a solid-state reaction method. The diffusion doping of $\text{Bi}_{1.8}\text{Pb}_{0.35}\text{Sr}_{1.9}\text{Ca}_{2.1}\text{Cu}_3\text{O}_y$ by Au increased the critical current density from 40 to 125 A cm^{-2} and the critical transition temperature by about 4 K compared with the pure sample. Both the critical current density and critical transition temperature of the Au-doped samples were increased on increasing the diffusion-annealing duration. The lattice parameter c of Au-doped samples increased by about 0.19% while the lattice parameters a and b did not change significantly. In addition, Au doping increased the amount high- T_c phase, decreased the amount low- T_c phase and improved the surface morphology. It is observed that for diffusion of Au atoms in $\text{Bi}_{1.8}\text{Pb}_{0.35}\text{Sr}_{1.9}\text{Ca}_{2.1}\text{Cu}_3\text{O}_y$ in the temperature range 500–800 °C, the coefficient of diffusion increases from 2×10^{-10} to $1.2 \times 10^{-8} \text{ cm}^2 \text{ s}^{-1}$, the corresponding activation energy being 1.08 eV. The low value of the activation energy indicates that the Au diffusion proceeds through defects in the ceramic samples.

Acknowledgments

This work is supported partly by the Scientific and Technological Council of Turkey (Project No: 104T325) and partly by the Turkish State Planning Organization (DPT) (Project No: 2004K120200).

References

- [1] Dzhafarov T D, Altunbaş M, Varilci A, Küçükömeroğlu T and Nezir S 1996 *Solid State Commun.* **99** 839
- [2] Terzioğlu C, Yilmazlar M, Ozturk O and Yanmaz E 2005 *Physica C* **423** 119
- [3] Dzhafarov T D, Cömert H, Altunbaş M, Alver Ü, Küçükömeroğlu T and Kopya A I 1995 *J. Alloys Compounds* **221** 246
- [4] Nanda Kishore K, Muralidhar M and Hari Babu V 1993 *Physica C* **204** 299
- [5] Dzhafarov T D and Yilmazlar M 1997 *Physica C* **292** 140
- [6] Ilyushechkin A Y, Yamashita T, Boskovic L and Mackinnon I D R 2004 *Supercond. Sci. Technol.* **17** 1201
- [7] Biju A, Aloysius R P and Syamaprasad U 2005 *Supercond. Sci. Technol.* **18** 1854
- [8] Prabitha V G, Biju A, Abhilashkumar R G, Sarun P M, Aloysius R P and Syamaprasad U 2005 *Physica C* **433** 28
- [9] Li Y, Kaviraj S, Berenov A, Perkins G K, Driscoll J, Caplin A D, Cao G H, Ma Q Z, Wang B, Wei L and Zhao Z X 2001 *Physica C* **355** 51
- [10] Görür O, Küçükömeroğlu T, Terzioğlu C, Varilci A and Altunbaş M 2005 *Physica C* **418** 35
- [11] Görür O, Terzioğlu C, Varilci A and Altunbaş M 2005 *Supercond. Sci. Technol.* **18** 1233
- [12] Hua L, Yao G Z, Jiang M, Wang Y Z, Tang H and Li Z R 1995 *J. Appl. Phys.* **78** 3274
- [13] Yu Y *et al* 1995 *Phys. Status Solidi* **151** k9
- [14] Matsushita T, Suzuki A, Kishida T, Okuda M and Naito H 1994 *Supercond. Sci. Technol.* **7** 222
- [15] Cömert H, Altunbaş M, Dzhafarov T D, Küçükömeroğlu T, Asadov Y G and Karal H 1994 *Supercond. Sci. Technol.* **7** 824
- [16] Jeong D Y, Sohn M H and Ha D W 1991 *Physica C* **85–89** 2487
- [17] Jin S, Sherwood R C, Tiefel T H and Kammlott G W 1998 *Appl. Phys. Lett.* **52** 1628
- [18] Liu H K, Dou S X, Song K H and Sorrell C C 1990 *Supercond. Sci. Technol.* **3** 210
- [19] Grivel J C and Flukiger R 1994 *Physica C* **229** 177
- [20] Yilmazlar M, Ozturk O, Görür O, Belenli I and Terzioğlu C 2007 *Supercond. Sci. Technol.* **20** 365
- [21] Ozturk O, Nursoy M, Terzioğlu C and Belenli I 2007 *J. Alloys Compounds*. at press
- [22] Chiu C W, Meng R L, Gao L, Huang Z J, Chen F and Xue Y Y 1993 *Nature* **365** 323
- [23] Halim S A, Khawaldeh S A, Mohammed S B and Azhan H 1999 *Mater. Chem. Phys.* **61** 251
- [24] Dzhafarov T D 1996 *Phys. Status Solidi a* **158** 335
- [25] Dzhafarov T D, Altunbaş M, Varilci A and Küçükömeroğlu T 1995 *Mater. Lett.* **25** 81
- [26] Abdullaev G B and Dzhafarov T D 1987 *Atomic Diffusion in Semiconductor Structures* (New York: Harwood–Academic)
- [27] Persland M R, Tallon J L, Buckley R G, Liu R S and Floer N E 1991 *Physica C* **176** 95
- [28] Aksan M A and Yakinci M E 2004 *J. Alloys Compounds* **385** 33